Supporting Information for the Paper Entitled:

Crystalline Coordination Networks of Zero-Valent Metal Centers: Formation of a 3-Dimensional Ni(0) Framework with *m*-Terphenyl Diisocyanides

Douglas W. Agnew,[1] Ida M. DiMucci,[2] Alejandra Arroyave,[1] Milan Gembicky,[1] Curtis E. Moore,[1] Samantha N, MacMillan,[2] Arnold L. Rheingold,[1] Kyle M. Lancaster,[2] and Joshua S. Figueroa[1]*

[1] *Department of Chemistry and Biochemistry, University of California, San Diego, 9500 Gilman Dr., Mail Code 0358, La Jolla CA, 92093-0358. Email: jsfig@ucsd.edu*

[2] *Department of Chemistry and Chemical Biology, Cornell University, Ithaca, NY 14853, USA.*

Contents

S1. Synthetic Procedures

S1.0. General Considerations. All manipulations were performed under an atmosphere of dry dinitrogen using standard Schlenk and glovebox techniques, unless otherwise stated. Solvents were dried and degassed according to standard procedures. Reagent grade starting materials were purchased from commercial sources and used without further purification, unless otherwise stated. $CNAr^{Mes2}$ and $[CNAr^{Mes2}]_2$ were prepared as described previously.[1,2] Elemental analysis was performed by Midwest Microlabs, Inc. of Indianapolis, IN.

S1.1. Synthesis of Ni-^{ISO}CN-2. To a stirring solution of $Ni(COD)_2$ in THF (0.009 g, 0.033 mmol, 4 mL), was added a THF solution of $[CNAr^{Mes2}]_2$ (0.065 g, 0.096 mmol, 3.0 equiv., 4 mL) over a 5 min period, causing the formation and precipitation of a deep red powder. This mixture was stirred for 30 minutes at room temperature, after which it was transferred to a 15 mL pressure tube and capped with a Teflon screw-cap. The tube was then placed in a sand bath inside an oven set to 100 ˚C for a 48 h period, after which it was allowed to cool to room temperature over a 5 h period. The deep maroon solid was transferred to a scintillation vial and the supernatant was decanted off. Following two wash cycles (consisting of gentle agitation in 4 ml THF followed by decantation), all volatiles were removed under dynamic vacuum for 6 h to provide 0.037 g of a deep maroon, free-flowing solid. ATR-IR (solid sample): ν_{CN} = 2050 cm^{-1} (b).

S1.2. Preparation of Ni-^{ISO}CN-2·($[CNAr^{Mes2}]_2$)$_{0.5}$. Single crystals of Ni-^{ISO}CN-2·($[CNAr^{Mes2}]_2$)$_{0.5}$ were prepared as follows: $Ni(COD)_2$ (0.004 g, 0.0146 mmol) mechanically mixed with $[CNAr^{Mes2}]_2$ (0.059 g, 0.087 mmol, 6.0 equiv.) with a mortar and pestle, and the resulting solid mixture was transferred to a 15 mL pressure tube. To this mixture was added *ca*. 0.1 mL THF, and the tube was placed in a sand bath inside an oven set to 100 ˚C for one day, followed by cooling to room temperature over 24 h. The deep black/red cubic crystals thus prepared are amenable to analysis by single crystal X-ray diffraction. ATR-IR (solid sample): ν_{CN} = 2114(s, free $[CNAr^{Mes2}]_2$), 2050 cm^{-1} (b).

S1.3. Preparation of $[Ni(CNAr^{Mes2})_4]OTf$. To a stirring benzene solution of $Ni(CNAr^{Mes2})_4$ (0.054 g, 0.0379 mmol, 2 mL) was added a suspension of FcOTf (0.014 g, 1.1 eq.) in benzene. The dark red solution was allowed to stir for 4 hours at room temperature, during which time the solution lightened to yellow. The resultant solution was then filtered through a fiberglass plug, and all volatiles were removed under reduced pressure. The dark yellow solid obtained was then washed with pentane (5 x 5 mL) to remove ferrocene, providing a light yellow solid. The product was then placed under dynamic vacuum for 3 h to remove trace solvent. Yield 0.055 g, 93%. X-ray quality crystals were grown from a concentrated toluene solution at –35 ˚C over 2 days. ^{1}H NMR (400.1 MHz, C_6D_6, 20 ˚C) δ = 8.48 (br s), 6.60 (br s), 2.40 (br s), 2.11 (br s) ppm. FTIR (C_6D_6, KBr windows): ν_{CN} = 2147 cm^{-1} (w,sh), 2105 cm^{-1} (vs), also 2957, 2921, 2859, 1614, 1312, 1253, 1233, 1211, 1611, 1050, 847, 757 cm^{-1}. Evans Method: μ_{eff} (C_6D_6 with $(Me_3Si)_2O$ reference, 500.2 MHz, 20 ˚C, 3 runs) = 1.84 (±0.15) μ_B. Anal. Calcd for $C_{101}H_{100}F_3N_4NiO_3S$: C, 77.48; H, 6.44; N, 3.58. Found C, 77.63; H, 6.33; N, 3.42.

S2. X-ray Absorption Spectroscopy (XAS) Studies

S2.1. Experimental details. Data collection at SSRL on 9-3. Ni K-edge XAS spectra were collected on the 16 pole, 2 T wiggler beamline 9-3 at the Stanford Synchrotron Radiation Lightsource (SSRL) under ring conditions of 3 GeV and 500 mA. Samples were diluted in BN, pressed into 1 mm aluminum spacers and sealed with 37 μm Kapton tape. Samples were maintained at 10 K in a liquid He cryostat during data collection. A Si(220) double-crystal monochromator was used for energy selection and a Rh-coated mirror (set to an energy cutoff of 13 keV) was used for harmonic rejection. Internal energy calibration was performed by assigning the first inflection point of a Ni foil spectrum to 8331.6 eV. Data on samples $Ni(CNAr^{Mes2})_4$, $[Ni(CNAr^{Mes2})_4]OTf$, $Ni(COD)_2$ (as a control for Ni(0)), and Ni-^{ISO}CN-2 were collected in fluorescence mode with a Lytle detector. For spectra measured by fluorescence detection, elastic scatter into the detector was attenuated using a Soller slit with an upstream Co filter.

S2.2. Data Processing. The raw data were averaged and energy shifted using Igor. Data were calibrated using an internal Ni foil standard. Spectra were shifted such that the Ni foil rising edge inflection point matched the value of 8331.6 eV (EXAFSPAK).[3] The averaged data file was then normalized and corrected in SixPACK[4] by applying a linear normalization for the pre-edge and a quad normalization for the post-edge to produce the final spectra

S2.3. Calculations. All electronic structure and spectroscopic calculations were performed using the ORCA computational chemistry package.[5] Geometry optimizations were performed using the BP86[6] functional, the zeroth-order regular approximation for relativistic effects (ZORA)[7,8] as implemented by van Wüllen[9], and the CP(PPP)[10] basis set. Optimized coordinates, as well as crystal structures when available, were used for TDDFT[11] calculations of Ni K-edge XAS utilizing the B3LYP[12] functional. For the TDDFT calculations of $[Ni(CNAr^{Mes2})_4]OTf$, the Ar^{Mes2} group of isocyanide ligand was truncated to a 2,6-dimethylphenyl group to allow for energy convergence. Calculated excitation energies were plotted against experimental energies for the B3LYP functional. These fits were used to shift the calculated energy of the spectra and produce calculated spectra that correlate well to experimental spectra.

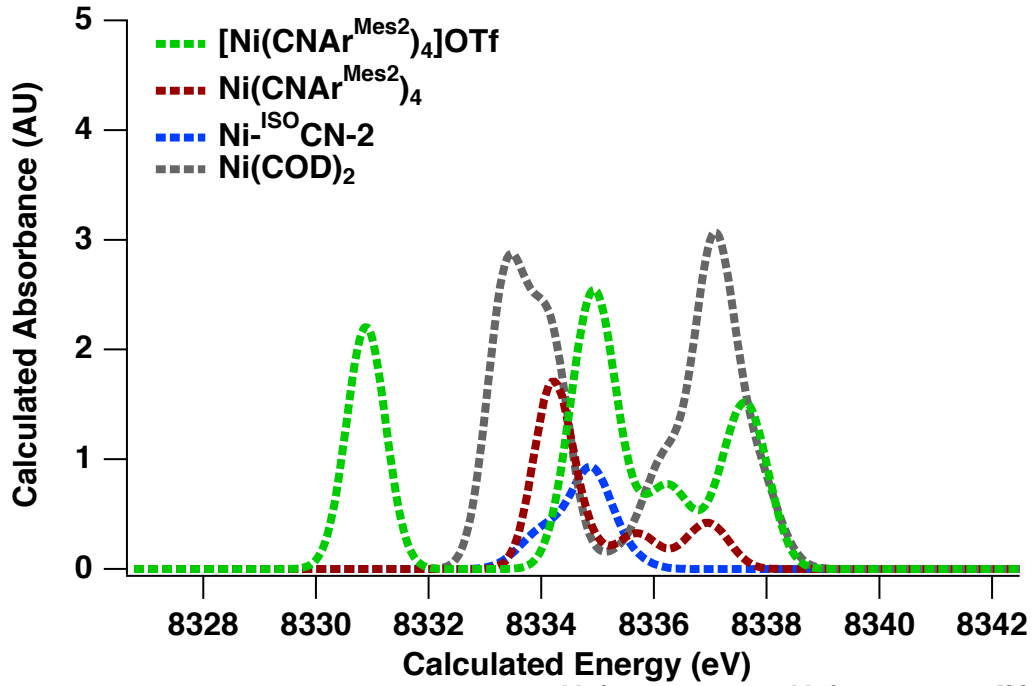

Figure 2.1. Calculated spectra for $Ni(CNAr^{Mes2})_4$, $[Ni(CNAr^{Mes2})_4]OTf$, Ni-^{ISO}CN-2, and $Ni(COD)_2$ (COD = 1,5-cyclooctadiene). Energy is adjusted based on correlation curve in Figure 2.2.

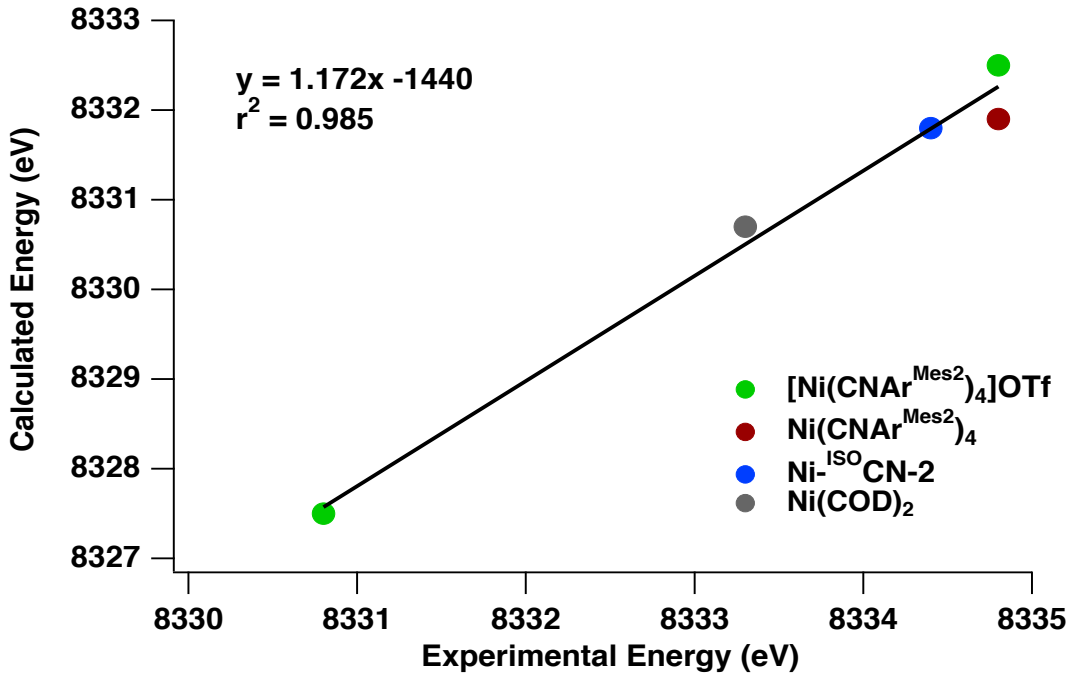

Figure 2.2. Correlation curve of experimentally collected pre-edge energy to B3LYP calculated energy for $Ni(COD)_2$, $Ni(CNAr^{Mes2})_4$, $[Ni(CNAr^{Mes2})_4]OTf$, and Ni-^{ISO}CN-2, used to shift calculated spectra. Note, only $[Ni(CNAr^{Mes2})_4]OTf$, which is formally Ni(I), shows an additional low-energy pre-edge transition.

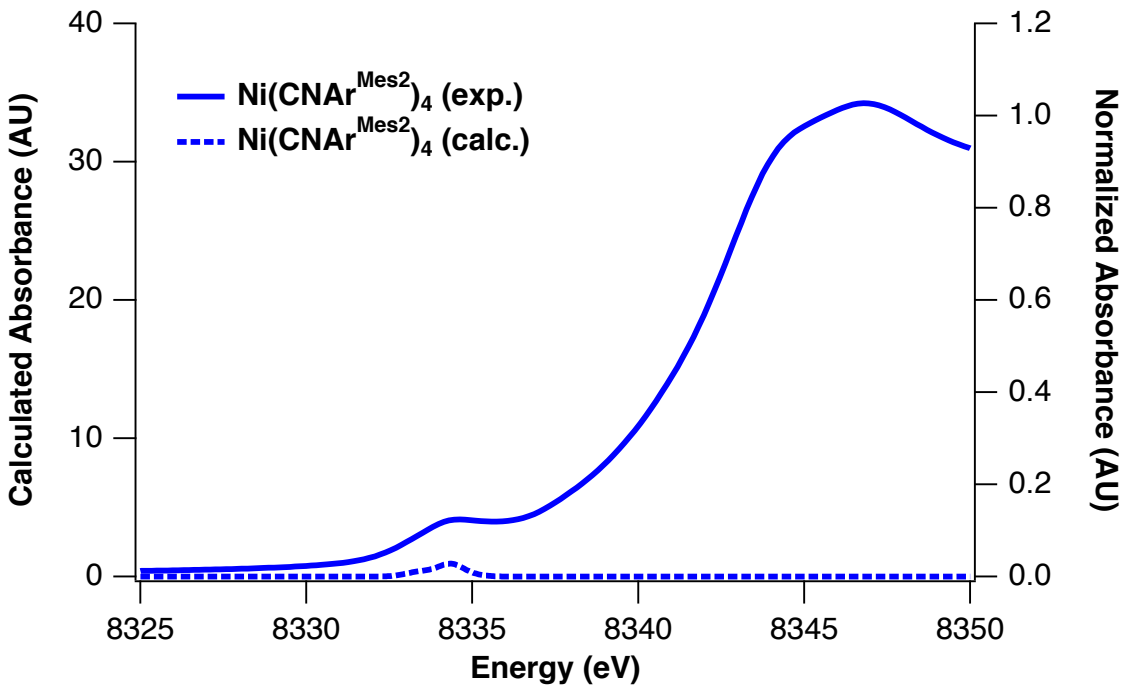

Figure 2.3. Comparison of B3LYP calculated spectra and experimentally obtained spectra of compound $Ni(CNAr^{Mes2})_4$.

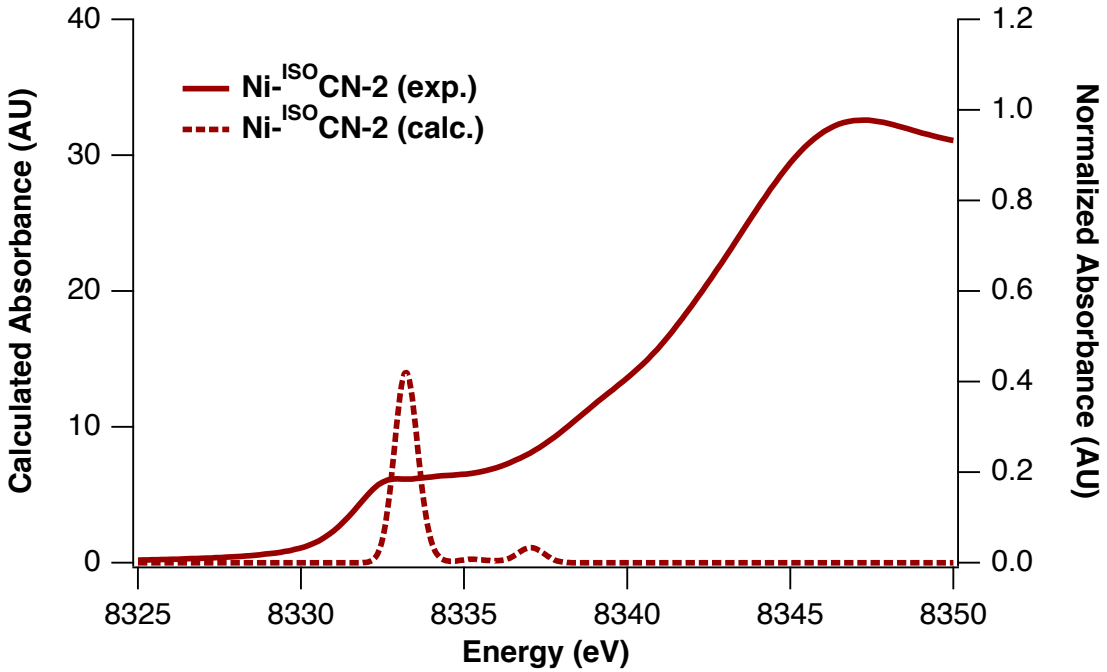

Figure 2.4. Comparison of B3LYP calculated spectra and experimentally obtained spectra of compound Ni-^{ISO}CN-2.

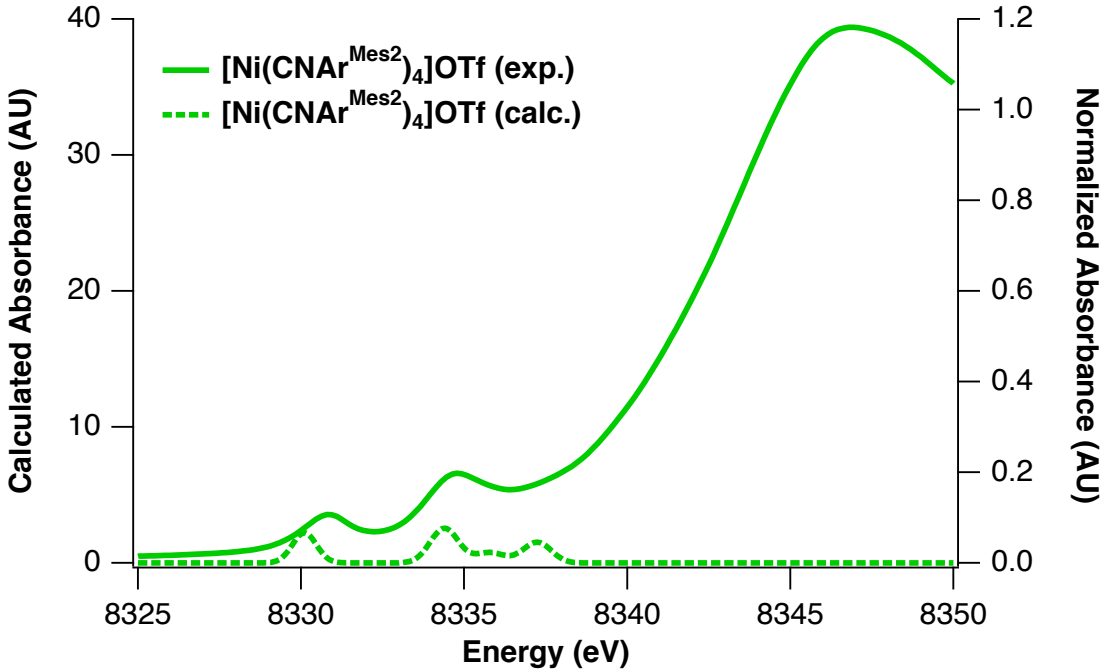

Figure 2.5. Comparison of B3LYP calculated spectra and experimentally obtained spectra of compound [Ni(CNAr^{Mes2})$_4$]OTf.

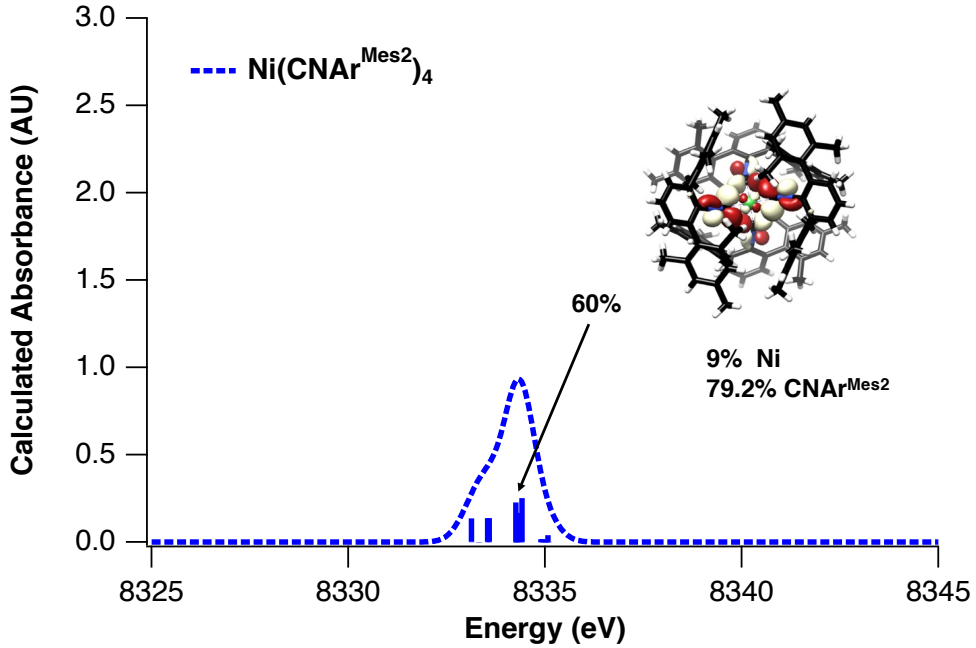

Figure 2.6. B3LYP calculated transitions and accepting molecular orbitals for Ni(CNAr^{Mes2})$_4$.

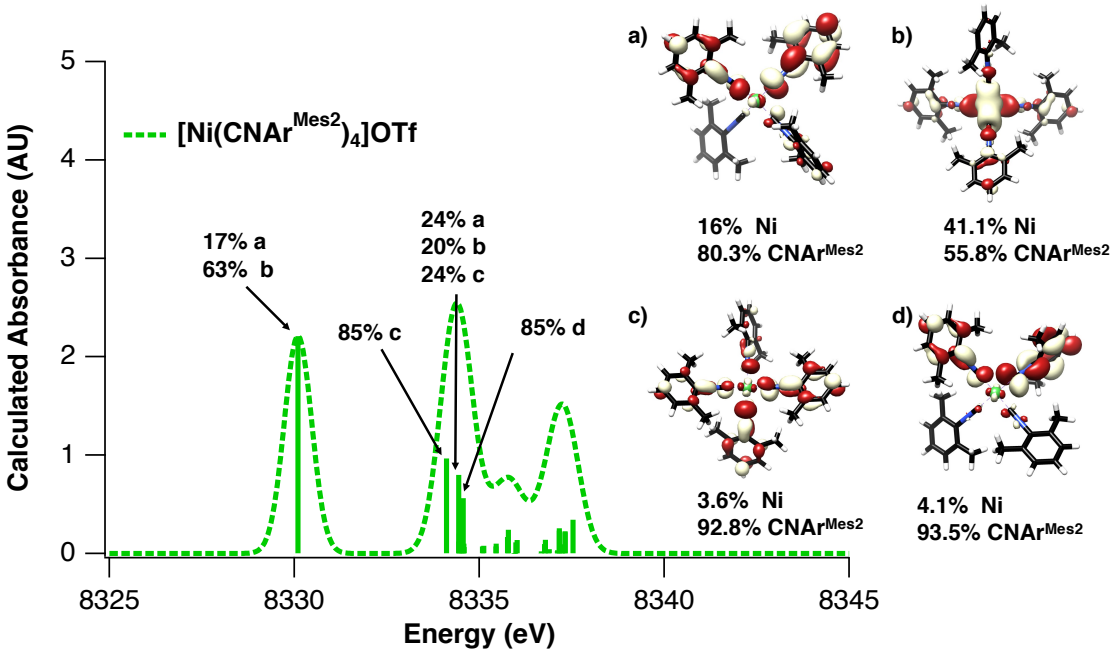

Figure 2.7. B3LYP calculated transitions and accepting molecular orbitals for [Ni(CNAr^{Mes2})$_4$]OTf.

S3. Crystallographic Structure Determinations

S3.1. General. Single X-ray structure determinations were performed at 100 K on Bruker Kappa Diffractometers equipped with either Cu-Kα or Mo-Kα radiation sources and an APEX-II CCD area detector. All structures were solved *via* direct methods with SHELXS[13] and refined by full-matrix least-squares procedures using SHELXL[1] within the Olex2[14] software. In cases of highly disordered solvent molecules, the Platon routine SQUEEZE[15] was used to account for the corresponding electrons as a diffuse contribution to the overall scattering without specific atom positions. Crystallographic data collection and refinement information is listed in Table S3.1.

Notes on Structure Solutions

Ni-^{ISO}CN-2·([CNAr^{Mes2}]$_2$)$_{0.5}$: Three mesityl rings were found to be positionally disordered and were modeled and refined anisotropically. Free [CNAr^{Mes2}]$_2$ and a THF solvent molecule were modeled at 50% occupancy in the void space. This resulted in a higher wR_2 value than if the corresponding electron density was treated with SQUEEZE and removed; however, inclusion of these modeled components was determined to provide a more accurate description of the structure. Residual electron density which could not be satisfactorily modeled was then treated with SQUEEZE and its electron density removed.

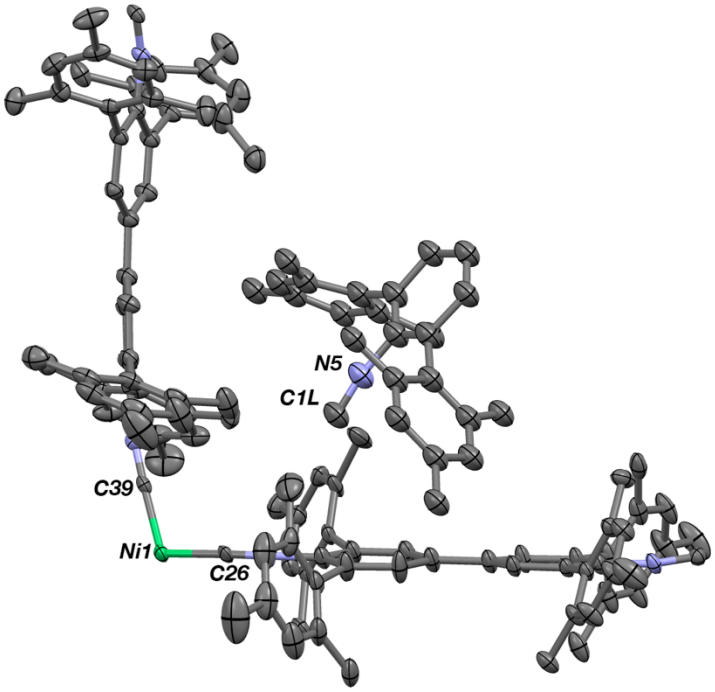

Figure S3.1. Asymmetric unit of Ni-^{ISO}CN-2·([CNAr^{Mes2}]$_2$)$_{0.5}$, with THF solvent molecule and disordered mesityl rings omitted for clarity.

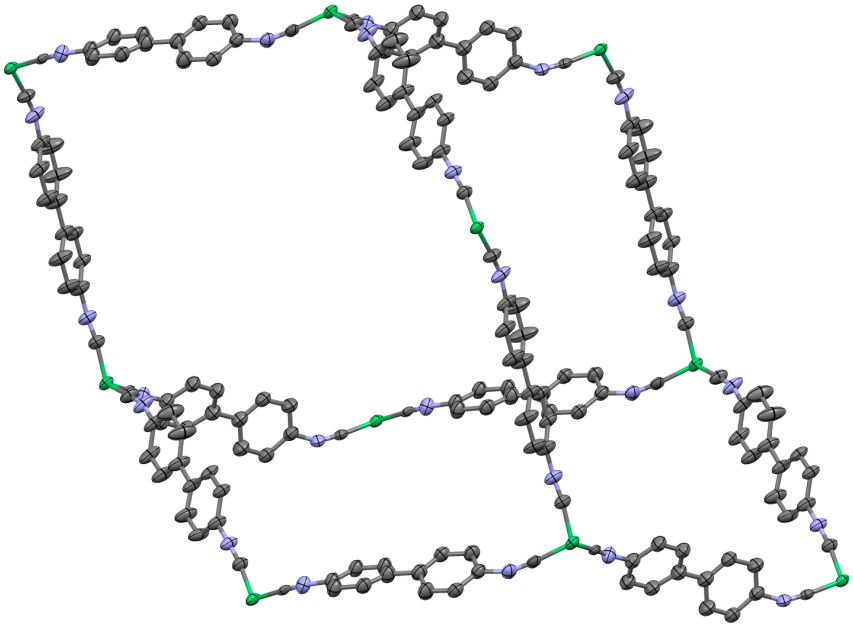

Figure S3.2. Diamondoid architecture generated by tetra-coordinated Ni(0) nodes in Ni-^{ISO}CN-2·([CNAr^{Mes2}]$_2$)$_{0.5}$.

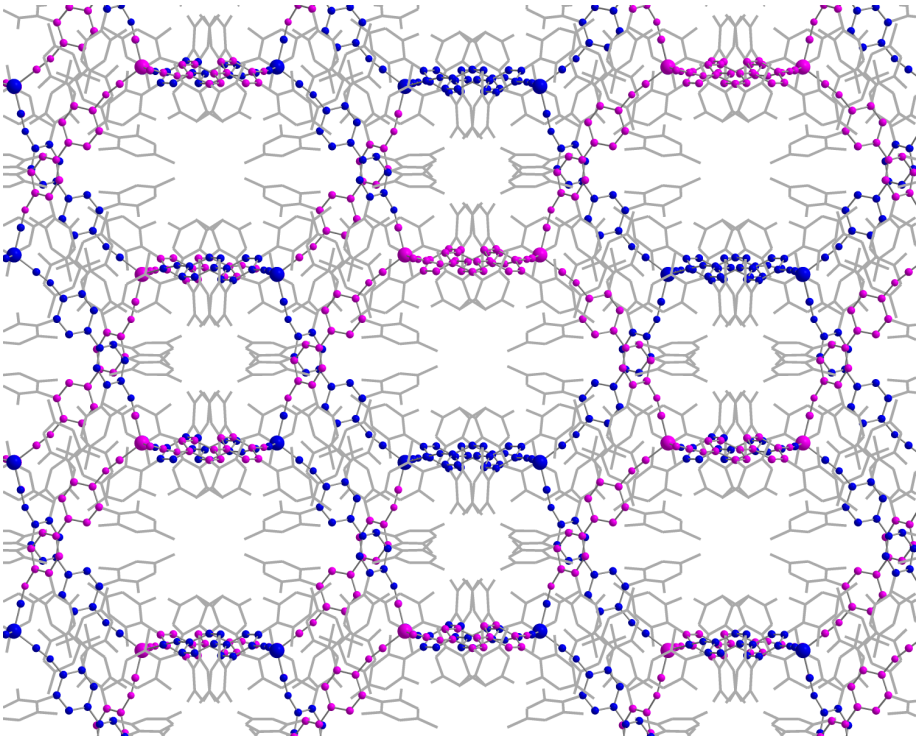

Figure S3.3. View of Ni-^{ISO}CN-2·([CNAr^{Mes2}]$_2$)$_{0.5}$ along the *001* axis, showing the interpenetration of the two independent lattices.

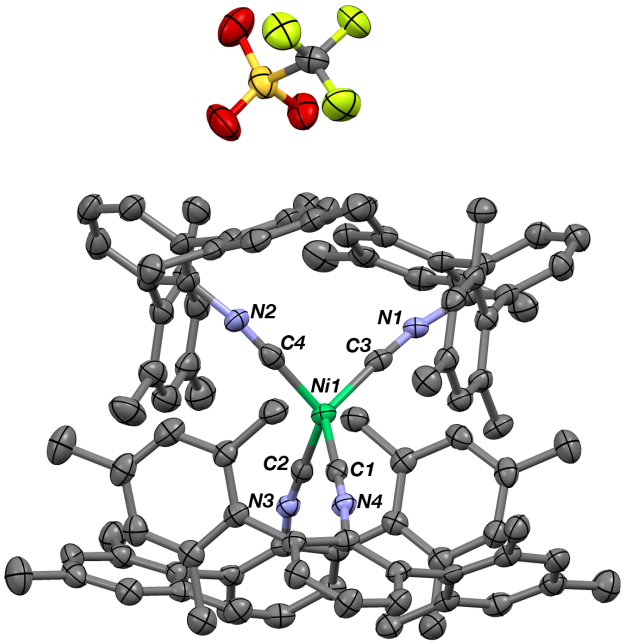

Figure S3.4. Molecular structure of [Ni(CNAr^{Mes2})$_4$]OTf, with toluene solvent molecule of co-crystallization omitted. Selected bond distances (Å) and angles (°): Ni1-C1 = 1.916(4); Ni1-C3 = 1.924(4); Ni1-C2 = 1.917(5); Ni1-C4 = 1.902(5); N3-C2 = 1.152(5); C4-Ni1-C3 = 130.08(16); C1-Ni1-C2 = 97.69(16); C2-Ni1-C3 = 104.72(16); C4-Ni1-C1 = 103.61(17); C4-Ni1-C3 = 98.61(17); C4-Ni1-C2 = 125.47(17).

Table S3.1

Name	Ni-^{ISO}CN-1·([CNAr^{Mes2}]$_2$)$_{0.5}$	[Ni(CNAr^{Mes2})$_4$]OTf·C_7H_8
Formula	$C_{114.29}H_{111.62}N_{4.5}NiO_{0.5}$	$C_{108}H_{108}F_3N_4NiO_3S$
Crystal System	Monoclinic	Monoclinic
Space Group	*C*2/*c*	$P2_1/c$
a, Å	29.5994(12)	16.5352(6)
b, Å	34.1170(11)	21.4824(9)
c, Å	25.9158(9)	24.9074(11)
α, deg	90	90
β, deg	124.556(2)	94.939(2)
γ, deg	90	90
V, Å^3	21553.6(14)	8814.7(6)
Z	2	4
Radiation (λ, Å)	Cu-Kα, 1.54178	Mo-Kα, 0.71073
ρ (calcd.), Mg/m^3	0.995	1.249
μ (Mo Ka), mm^{-1}	0.595	0.309
Temp, K	100	100
θ max, deg	50.589	25.489
data/parameters	11351/1086	16252/1106
R_1	0.0982	0.0676
wR_2	0.2507	0.1550
GOF	0.987	1.022

S4. IR spectra and PXRD Patterns

S4.0. Experimental details. Solid-state IR spectra were collected at 2 cm^{-1} resolution using a Bruker Platinum Alpha ATR-IR equipped with a diamond crystal. Air-free analyses were collected using this instrument inside a nitrogen-filled glovebox. The following abbreviations are used to describe the intensity and characteristics of important IR absorption bands: vs = very strong, s = strong, m = medium, w = weak, vw = very weak, b = broad, vb = very broad, sh = shoulder.

Low-temperature powder X-ray diffraction was collected using Cu-Kα radiation (λ = 1.54178 Å) on a Bruker Kappa diffractometer equipped with a VÅNTEC-500 area detector and an Oxford Cryostream 700, and were collected to 2θ = 45˚. Samples were prepared on a nylon loop using minimal Paratone oil. Crystalline material, as prepared, was used without grinding to preserve structural integrity; we therefore believe discrepancies in peak intensity are due to preferential orientation of the crystallites. Corrections for the anomalous scattering caused by the nylon loop and Paratone oil were performed by subtracting a background scan consisting solely of these materials. The experimental background of the collected patterns was corrected using the DIFFRAC.SUITE EVA software package from Bruker Corporation.

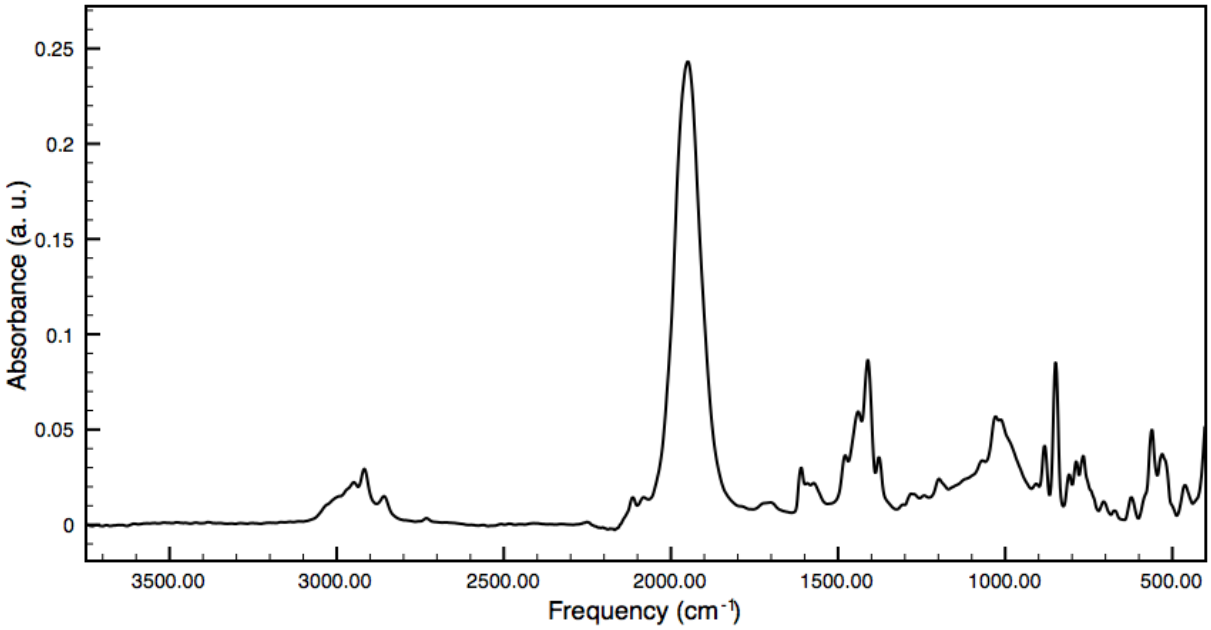

Figure S4.1. Solid-state ATR-IR spectrum of Ni-^{ISO}CN-2 with a dominant ν_{CN} band centered at 1950 cm^{-1}.

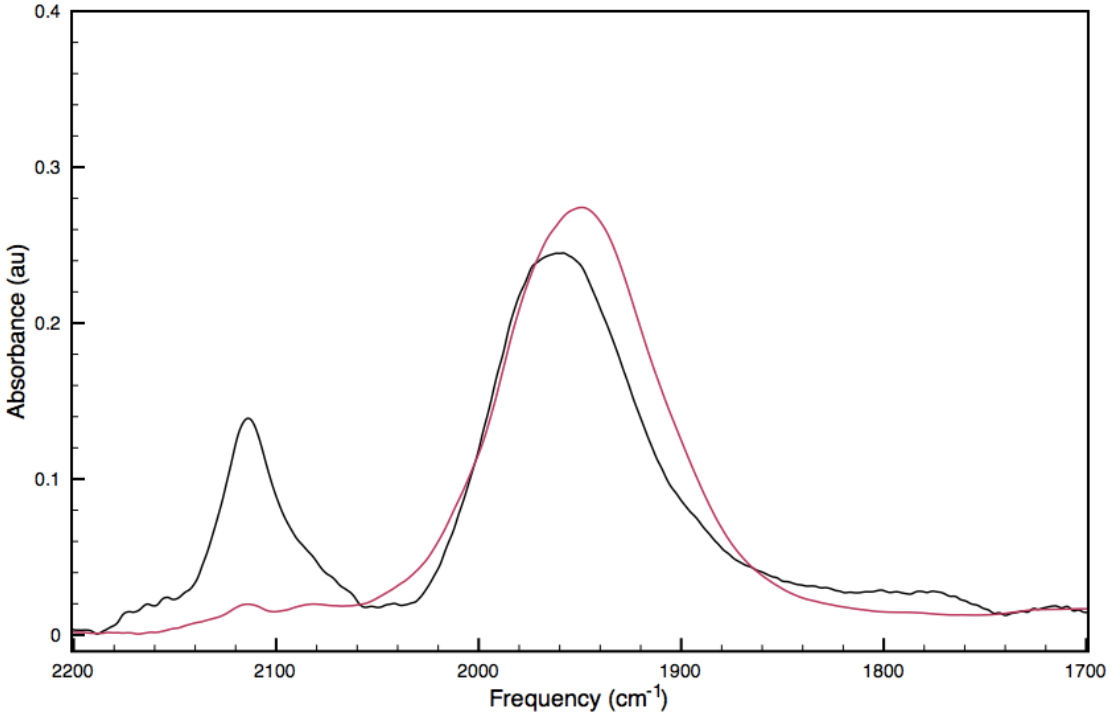

Figure S4.2. Comparative overlay of ATR-IR spectra of Ni-^{ISO}CN-2 (red) and Ni-^{ISO}CN-2·([CNAr^{Mes2}]$_2$)$_{0.5}$ (black). Note, free [CNAr^{Mes2}]$_2$ displays the ν_{CN} band at 2114 cm^{-1}.

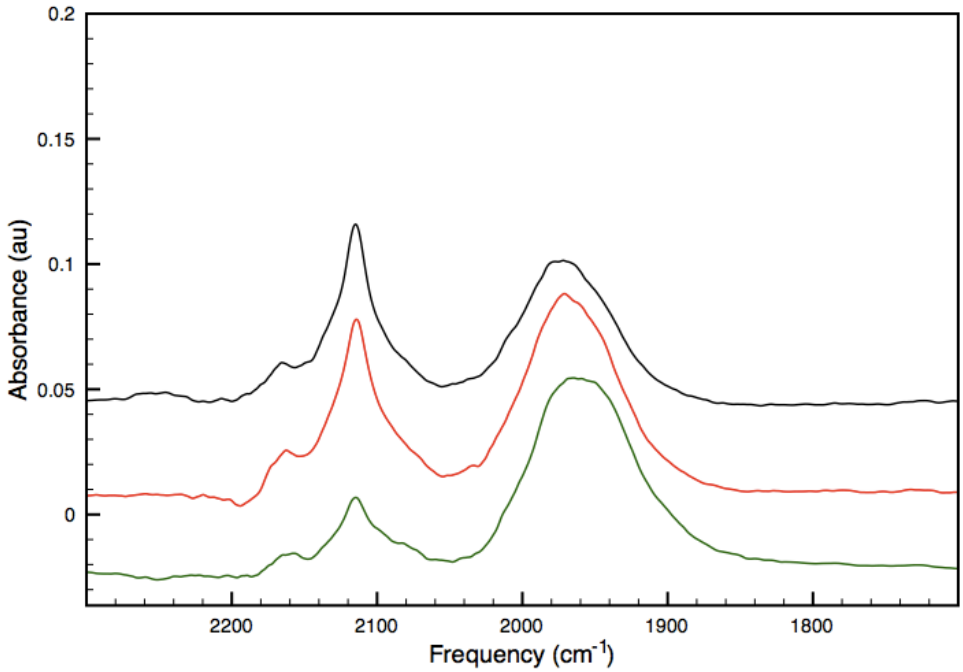

Figure S4.3. ATR-IR spectra of solid Ni-^{ISO}CN-2 after exposure to ambient atmosphere (30 s (green); 24 h (red); 5 days (black)) showing degradation to free [CNAr^{Mes2}]$_2$ (ν_{CN} = 2114 cm^{-1}) over time.

S5. Thermogravimetric Analysis (TGA) and Porosimetry Measurements

S5.1. Thermal Analysis. Thermogravimetric analysis (TGA) was performed in a pre-weighed alumina crucible, which was loaded with material under a dinitrogen atmosphere. The crucible was transferred under a blanket of Ar gas to the TGA instrument. Analysis was conducted under a stream of dry dinitrogen gas (80 mL/min) using a Mettler Toledo TGA/DSC 1 STARe System running from 30 ˚C to 800 ˚C with a ramping rate of 5 ˚C/min.

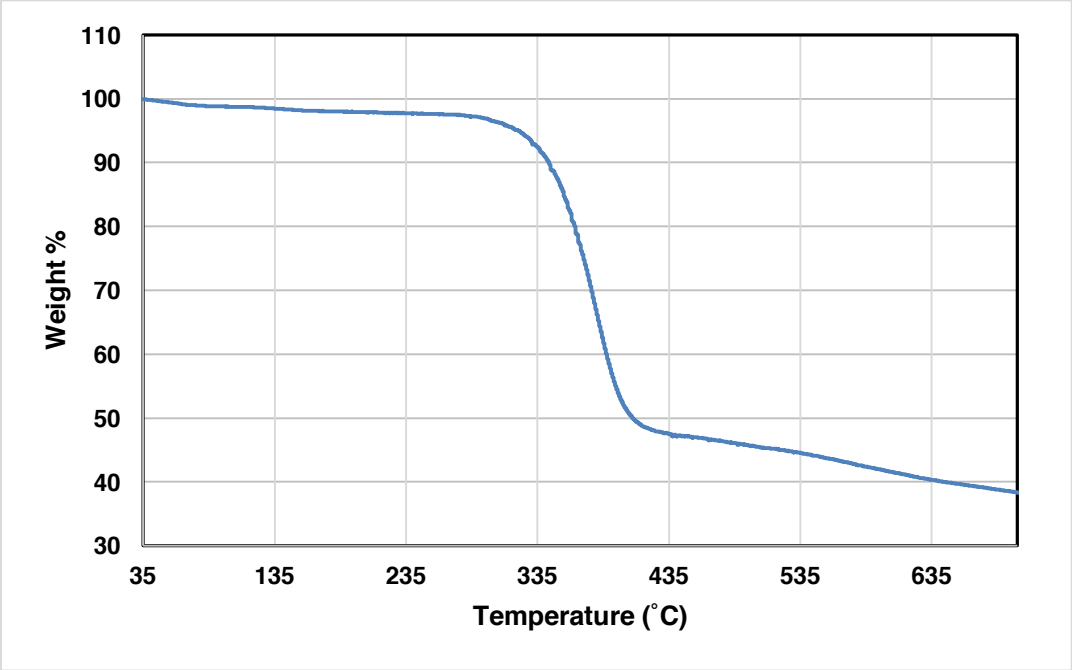

Figure S5.1. TGA trace for Ni-^{ISO}CN-2. The large weight degradation has an onset temperature of 302 ˚C.

S5.2. Surface Area Analysis. Samples were prepared on and measured using a Micrometrics ASAP 2020 Adsorption Analyzer. Approximately 40 mg of material was transferred to a pre-weighed sample tube in an Ar-filled glovebox and degassed at 80 ˚C for at least 10 hours or until the outgas rate was below 5 mmHg. The sample tube was reweighed to obtain a mass for the sample. Measurements were collected on three independent samples at 77 K employing N_2 of 99.999% purity using the volumetric technique. N_2 adsorption isotherms for Ni-^{ISO}CN-2 are shown in Figure 4 of the text. N_2 adsorption isotherms for Ni-^{ISO}CN-2·([CNAr^{Mes2}]$_2$)$_{0.5}$ are shown in Figure S5.2 below.

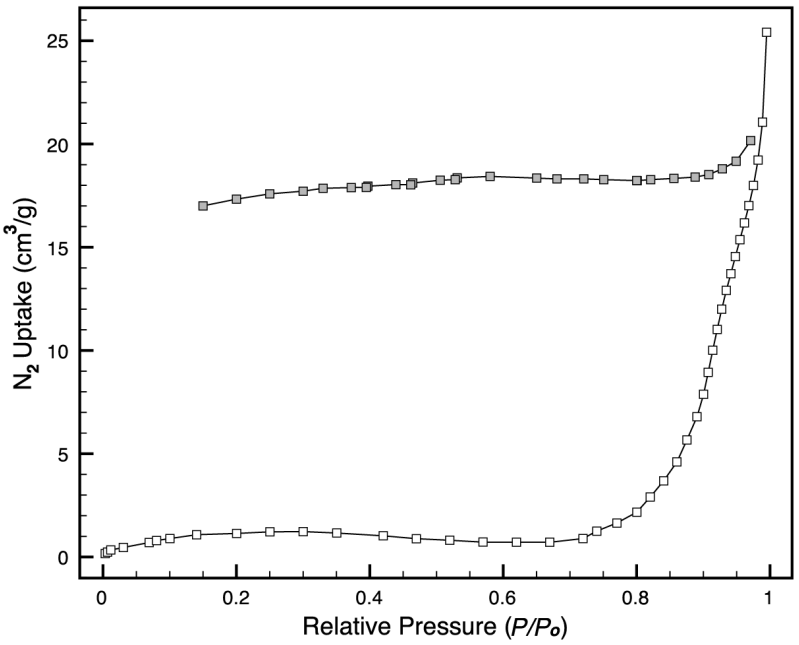

Figure S5.2. N_2 adsorption isotherms (77 K) for Ni-^{ISO}CN-2·([CNAr^{Mes2}]$_2$)$_{0.5}$ showing negligible gas uptake; white boxes = absorption, grey boxes = desorption.

S6. Accessible Surface-Area Calculations

S6.1. General. The accessible surface area was calculated using the Monte Carlo integration technique introduced by Düren and co-workers.[16,17] The diameters of the framework atoms were taken from UFF force fields as outlined previously.[16] A standard diameter of N_2 of 3.681 Å was also employed.[16] The input CIF file used for this calculation was a modified version of the crystal structure obtained for Ni-^{iso}CN-2·[(CNAr^{Mes2})$_2$]$_{0.5}$, where reflections for free ligand in the pore was removed using the SQUEEZE[15] of the PLATON program suite. This model was used to approximate the internal morphology of Ni-isoCN-2. The Fortran 90 code used for the calculation was compiled on a home-built Linux system. The calculation on this model resulted in an accessible surface area of 492 m^2/g, which is within error of the experimental value for Ni-^{iso}CN-2 (580 m^2/g).

References

(1) B. J. Fox, Q. Y. Sun, A. G. DiPasquale, A. R. Fox, A. L. Rheingold, J. S. Figueroa, *Inorg. Chem.* **2008**, *47*, 9010-9020.

(2) Agnew, D. W.; Gembicky, M.; Moore, C. E.; Rheingold, A. L.; Figueroa, J. S. *J. Am. Chem. Soc.* **2016**, *138*, 15138-15141.

(3) George, G. N. *EXAFSPAK*; Stanford Synchrotron Radiation Lightsource, Stanford Linear Accelerator Center; Stanford University: Stanford, CA, 2001.

(4) Webb, S. *SIXPACK*; Stanford Synchrotron Radiation Lightsource, Stanford Linear Accelerator Center, Stanford University: Stanford, CA, 2002.
(5) Neese, F. *WIREs Comput. Mol. Sci.* **2012**, 2, 73−78.
(6) (a) Becke, A. D. *Phys. Rev. A: At., Mol., Opt. Phys.* **1988**, 38, 3098−3100. (b) Perdew, J. *P. Phys. Rev. B: Condens. Matter Mater. Phys.* **1986**, 33, 8822−8824.
(7) (a) Weigend, F.; Ahlrichs, R. *Phys. Chem. Chem. Phys.* **2005**, 7, 3297−3305. (b) Pantazis, D. A.; Chen, X.-Y.; Landis, C. R.; Neese, F. J. Chem. *Theory Comput.* **2008**, 4, 908−919.
(8) van Lenthe, E.; van der Avoird, A.; Wormer, P. E. S. *J. Chem. Phys.* **1998***,* 108, 4783−4796.
(9) van Wüllen, C. *J. Chem. Phys.* **1998**, 109, 392−399.
(10) Neese, F. *Inorg. Chim. Acta* **2002**, 337, 181−192.
(11) DeBeer George, S.; Petrenko, T.; Neese, F. *J. Phys. Chem. A* **2008,** 112, 12936−12943.
(12) Stephens, P.; Devlin, F.; Chabalowski, C.; Frisch, M. J. *J. Phys. Chem.* **1994**, 98, 11, 623−11627.
(13) Sheldrick. G. M. *Acta Crystallogr. A*. **2008**, 64, 112.
(14) Dolomanov, O. V.; Bourhis, L. J.; Gildea, R. J.; Howard, J. A. K.; Puschmann, H. J. *Appl. Cryst.* **2009**, 42, 339.
(15) van der Sluis, P.; Spek. A. L. *Acta Crystallogr*. **1990**, A46, 194-201.
(16) Düren, T.; Millange, F.; Ferey, G.; Walton, K. S.; Snurr, R. Q. *J. Phys. Chem. C* **2007**, *111*, 15350-15356.
(17) For the source code for Düren-type Accessible Surface Area calculations, see: www.see.ed.ac.uk/~tduren/research/surface_area/